



Applied Catalysis B: Environmental

journal homepage: www.elsevier.com/locate/apcatb



RF-plasma pretreatment of surfaces leading to TiO₂ coatings with improved optical absorption and OH-radical production

O. Baghriche^a, S. Rtimi^a, C. Pulgarin^{a,**}, C. Roussel^b, J. Kiwi^{c,*}

^a Ecole Polytechnique Fédérale de Lausanne, EPFL-SB-ISIC-GPAO, Station 6, CH-1015 Lausanne, Switzerland

^b Ecole Polytechnique Fédérale de Lausanne, EPFL SB SCGC-GE, Station 6, CH-1015 Lausanne, Switzerland

^c Ecole Polytechnique Fédérale de Lausanne, EPFL-SB-ISIC-LPI, Bat Chimie, Station 6, CH-1015 Lausanne, Switzerland

ARTICLE INFO

Article history:

Received 16 July 2012

Received in revised form 15 October 2012

Accepted 22 October 2012

Available online 1 November 2012

Keywords:

Vacuum RF-plasma

TiO₂ photocatalysis

OH-radicals

Bacterial inactivation kinetics

ABSTRACT

Evidence presented for the RF pretreatment of polyester enhances the TiO₂ coating generation of oxidative species/radicals under a low level actinic light irradiation. After 30 min RF-plasma pretreatment of the polyester samples, the fastest bacterial inactivation was observed concomitant with (a) the largest ratio of surface oxidized to the reduced functionalities as determined by XPS, (b) a strong sample optical absorption as seen by DRS and (c) the highest concentration surface OH-radicals monitoring the fluorescence of the hydroxy-terephthalic acid. Evidence for the photocatalyst self-cleaning was found by XPS due to the lack of accumulation of bacterial residues on the polyester-TiO₂. A further proof of self-cleaning was the ability by the polyester-TiO₂ samples to inactivate again bacterial charge at the end of an inactivation cycle. By XPS evidence is presented for the Ti⁴⁺/Ti³⁺ related redox catalysis and the details of the C and O-functionalities. Surface techniques such as XRF, DRS, TEM, contact angle (CA), XRD and XPS were applied to relate the microstructure of the TiO₂ coatings with the destruction of *Escherichia coli* taken as a probe.

© 2012 Elsevier B.V. All rights reserved.

1. Introduction

Semiconductors like TiO₂ and metal-semiconductor films like Ag/TiO₂ and Cu/TiO₂ films have been reported during the last decade to be effective in self-cleaning processes and bacterial inactivation kinetics [1,2]. Films to reduce/eliminate bacterial infections become nowadays increasingly important to preclude the formation of biofilms spreading bacteria for which antibiotics are not yet available and inducing [3–5] hospital acquired infections (HAI) [6,7]. TiO₂ photocatalysis [8–11] by way of TiO₂ coated textiles and TiO₂-Ag textile/polymers have been reported in the last decade leading to bacterial inactivation in the dark and under light irradiation [12–17].

Several laboratories have addressed the activation of substrates by RF-plasma to increase the binding of TiO₂ on different substrates [18–24]. Our group has reported the use of RF-plasma since 2003 to introduce certain functional groups as potential binding sites for TiO₂ and nano-metals and also to increase the textile hydrophilicity [11,17,18]. In subsequent studies we further reported the fixation

of TiO₂ and highly active nano-particulate antibacterial metals on a variety of substrates [23–29].

For the generation of RF-plasma, low pressures of 0.1–1 Torr are required to enhance the capture length of the electrons generated by the applied electric field. When applying vacuum in the RF-cavity the pressure is reduced and the O₂ left produces O^{*} and atomic O, singlet ¹O₂, anion-radicals O⁻ and cation-radicals like the O⁺. The collisions of the excited oxygen species with each other are drastically decreased by diminishing the number of initial molecules. This allows the O^{*} and atomic O in the RF-cavity to react with the polyester introducing oxidative functionalities [28–34]. In the plasma, the ions/molecules/electrons attain temperatures up to a few hundred degrees with high energies but lasting only nanoseconds in a system that is not in equilibrium. Within these short lifetimes, the plasma activates non-heat resistant textiles like polyester not damaging their structure and introducing oxygenated functionalities modifying the textile surface.

In the RF-cavity, the plasma discharge breaks the H–H and C–C bond scissions due to the non-uniform local heating of the fabric [30,31] segmenting partially the polyester fabric [32]. This interaction is sufficient to introduce the oxidative functionalities: –C–O⁻, –COO⁻, –COH⁻, O–C=O⁻, –COOH, phenolic and lactam groups in the presence of O₂ (air) [24,28–30]. These negative charged functionalities will react with the slightly positive Ti⁴⁺ charge of the TiO₂ by electrostatic attraction leading to surface coordination/chelation [26,27]. The TiO₂ nanocrystals

* Corresponding author. Tel.: +41 215348261; +41 216935690.

** Corresponding author. Tel.: +41 2169364720; +41 216935690.

E-mail addresses: cesar.pulgarin@epfl.ch (C. Pulgarin), john.kiwi@epfl.ch (J. Kiwi).

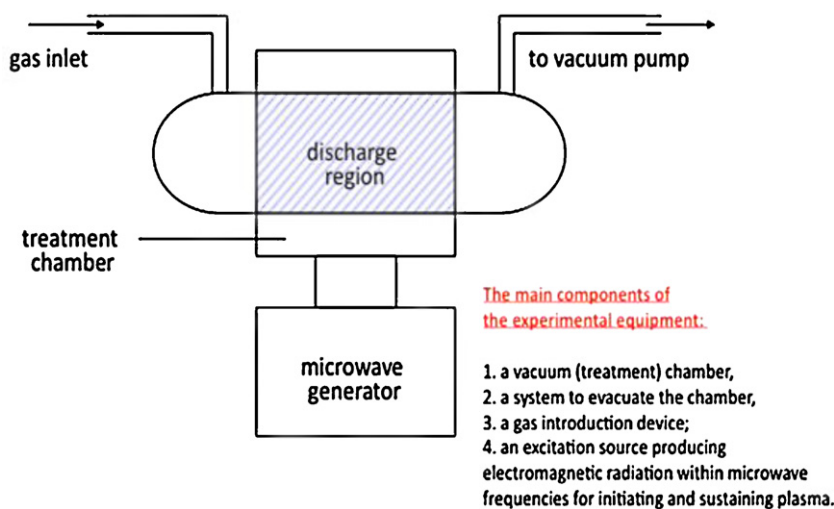


Fig. 1. Scheme of the RF-plasma unit used for the pretreatment of polyester samples.

will be attached to negatively charged substrates like Nafion by exchange/impregnation/electrostatic attraction as recently reported [33]. The attachment of the TiO_2 occurs for similar reasons to the ones taking place between the enhanced negative surface of polyester and the semiconductor due to the RF-pretreatment. Besides the functional oxygenated groups mentioned above, synthetic textile fibers have been reported to form a significant number of percarboxylate, epoxide, and peroxide groups upon RF-plasma pretreatment [3,21–23,31,35–37].

This study addresses (a) the enhanced deposition of TiO_2 on polyester pretreated by RF, (b) the use of low intensity visible/actinic light on the TiO_2 coated polyester leading to OH-radicals and their quantitative determination, (c) the optimization of the TiO_2 coating on the RF-pretreated polyester and (d) the bacterial inactivation kinetics on TiO_2 RF-plasma pretreated polyester.

2. Experimental

2.1. RF-plasma pretreatment of polyester textiles

The polyester used corresponds to the EMPA test cloth sample no. 407, polyester Dacron, type 54 spun, plain weave ISO 105-F04. The polyester fabrics were cleaned by a nonionic detergent solution at 80°C for 30 min to detach the stabilizers and impurities such as wax, fats, or additives. The polyester was then washed repeatedly with de-ionized water followed by immersion in ethanol, treated with ultrasonic for 5 min to remove organics and detergent residues and rinsed repeatedly with water and dried at 40°C [26].

In the second step the polyester fabric was pretreated in the vacuum cavity of the RF-plasma unit at around 1 Torr as shown in Fig. 1 (Harrick Corp. 13.56 MHz, 100 W). The topmost polyester layers up to 2 nm were RF-plasma pretreated for 10 min, 20 min, 30 min, 60 min and 120 min. Fig. 2 shows that the ratio of the oxidized species to reduced functionalities remained constant for pretreatment times above 30 min. This is the reason for the use of the RF-pretreated plasma sample for 30 min throughout this study.

2.2. Preparation of the TiO_2 Degussa P25 suspensions and loading of RF-pretreated polyester samples

The RF-plasma pretreated polyester samples $2\text{ cm} \times 2\text{ cm}$ were immersed in a sonicated TiO_2 Degussa P-25 suspension (5 g/L) and heated for 1 h at 75°C . Then the samples were heated at 100°C for 15 min. The loose bound TiO_2 was removed from the polyester

samples by sonication and the sample washed thoroughly with water and dried at 60°C [27,28]. Sometimes, this last step was repeated to deposit a second TiO_2 layer and obtain a more complete coverage of the polyester fabric. After the RF-pretreatment, the TiO_2 loading is immediately coated on the polyester since the functional groups and radicals introduced by RF-plasma on the polyester surface deactivate/hydrolyze rapidly due to the humidity and oxygen of the air [20,21].

2.3. X-ray fluorescence determination of the Ti weight percentage on polyester samples (XRF)

The Ti-content on the polyester was evaluated by X-ray fluorescence (XRF) since it emits an X-ray of a certain wavelength associated with its particular atomic number in the PANalytical PW2400 spectrometer. Table 1 shows the weight percentages of Ti on the polyester samples.

2.4. Evaluation of the bacterial inactivation of *Escherichia coli* and irradiation procedures

The samples of *E. coli* (*E. coli* K12) were obtained from the Deutsche Sammlung von Mikroorganismen und Zellkulturen GmbH (DSMZ) ATCC23716, Braunschweig, Germany. The bacterial evaluation method used has been reported previously to test the

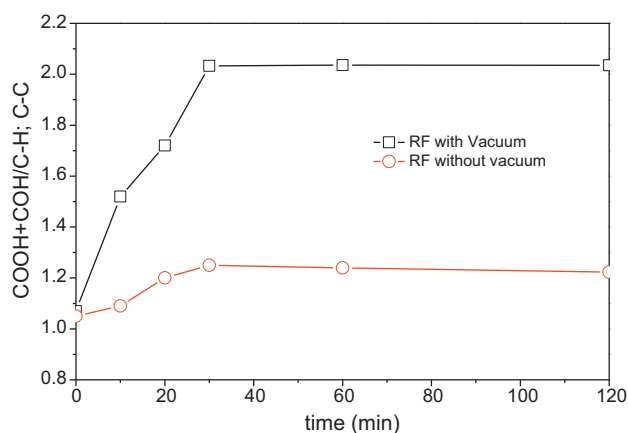


Fig. 2. Ratio of the main oxidized to reduced functionalities ($\text{COOH} + \text{COH}/\text{CH}-\text{CH}-$) introduced by RF on polyester as a function of pretreatment time t .

Table 1

Percentage weight of Ti on RF-treated samples as a function of treatment time determined by X-ray fluorescence.

| RF pretreatment time | % TiO ₂ (wt/wt) polyester | % Ti (wt/wt) polyester |
|----------------------|--------------------------------------|------------------------|
| 0 time | 0.345 | 0.201 |
| 10 min | 0.462 | 0.285 |
| 20 min | 0.621 | 0.341 |
| 30 min | 0.972 | 0.586 |
| 60 min | 0.978 | 0.588 |
| 120 min | 0.975 | 0.587 |

antibacterial activity of the Ti-polyester fabrics [9]. The bacterial data reported were replicated three times. To verify that no re-growth of *E. coli* occurs after the total inactivation observed in the first disinfection cycle, the samples were incubated for 24 h at 37 °C. Replica samples were incubated at 37 °C for 24 h at the end of each bacterial inactivation cycle. No bacterial re-growth was observed.

The irradiation of the polyester samples was carried out in a cavity provided with tubular Osram Lumilux 18 W/827 actinic light source. These lamps have a visible emission spectrum between 400 and 700 nm with an integral output of 1.0 mW/cm² resembling the light distribution found in solar irradiation.

2.5. Diffuse reflectance spectroscopy (DRS) of the RF-pretreated samples

Diffuse reflectance spectroscopy was carried out using a Perkin Elmer Lambda 900 UV–vis–NIR spectrometer provided for with a PELA-1000 accessory within the wavelength range of 200–800 nm and a resolution of one nm. The absorption of the samples was plotted in Kubelka–Munk (KM/S units) vs wavelength. “S” on Fig. 8 stands for the surface scattering of the sample.

2.6. Transmission electron microscopy (TEM) of TiO₂ polyester RF-pretreated samples

A Philips CM-12 (field emission gun, 300 kV, 0.17 nm resolution) microscope at 120 kV was used to visualize the TiO₂ coating on the polyester. The textiles were embedded in epoxy resin 45359 Fluka and the fabrics were cross-sectioned with an ultramicrotome (Ultracut E) at a knife angle at 35°.

2.7. X-ray diffraction (XRD) of the TiO₂-polyester RF-pretreated samples

The identification of the TiO₂ crystallographic phase anatase was carried out by means of an X'Pert diffractometer of the Philips, Delft, Netherlands. The K α line of Cu (1.5409 Å) radiation was used to reference the peak found.

2.8. Contact angle (CA) determination of the TiO₂-polyester RF-pretreated samples

Contact angles of the polyester samples as a function of the RF-plasma pretreatment time were assessed by means of a DataPhysics OCA 35 unit following the sessile method for water droplets.

2.9. X-ray photoelectron spectroscopy of TiO₂-polyester samples (XPS)

An AXIS NOVA photoelectron spectrometer (Kratos Analytical, Manchester, UK) equipped with monochromatic AlK α ($h\nu = 1486.6$ eV) anode was used during the study. The electrostatic charge effects on the samples were compensated by means of the low-energy electron source working in combination with a magnetic immersion lens. The carbon C1s line with position at

284.6 eV was used as a reference to correct the charging effect. The quantitative surface atomic concentration of some elements was determined from peak areas using sensitivity factors [38]. The spectrum background was subtracted according to Shirley [39]. The relative intensities of the XPS peaks depend on the spatial distribution of the emitting atoms inside the solid. Electrons with a defined energy E_0 loose energy due to inelastic scattering during the XPS analysis. This distorts the peak shape, height, intensity and the background of the XPS spectrum. Any XPS spectrum can be corrected for inelastic scattering if the depth profile, the inelastic mean free path and the inelastic cross section are known. For the elements reported in this study Ti, C, O, the inelastic cross section and the sensitivity factors allow to calculate the inelastic background, since the in-depth emitter profile is known [38,39]. For each element the Ti, C, O, the background subtraction and the intrinsic element peak can be obtained and used as reference for the quantitative analysis of the element XPS spectrum.

The XPS spectra for the Ti-species were analyzed by means of spectra deconvolution software (CasaXPS-Vision 2, Kratos Analytical UK). The deconvolution of the peaks was carried out by Gaussian–Lorentzian fitting of the peak shapes.

2.10. Detection of the OH-radical species on TiO₂ polyester using the fluorescence technique

The detection of the oxidative species (mainly OH-radicals) in the RF-plasma pretreated samples was carried out according to Hashimoto [40] and Girault [41]. Terephthalic acid 99% was purchased from ACROSS and the NaOH 98% was from Sigma Aldrich. A sample of 4 cm² of TiO₂ coated fabric was immersed in a solution made of terephthalic acid at 0.4 mM dissolved in a 4 mM NaOH solution. After each irradiation, the solution was transferred in a quartz cell and the fluorescence spectra of 2-hydroxyterephthalic acid generated by the reaction of terephthalic acid with the OH containing compound were measured on a Perkin Elmer LS-50B fluorescence spectrometer. The spectra were recorded between 300 and 600 nm (scan rate: 100 nm/min) under an excitation at 315 nm. The excitation and emission slits were fixed at 5 nm.

3. Results and discussion

3.1. Effect of the RF-pretreatment time of polyester samples on the amount of surface oxidized functionalities detected by XPS

Fig. 2 shows the effect of RF-plasma pretreatment time on polyester for 10 min, 20 min, 30 min, 60 min and 120 min. The changes in the concentration of the functional groups C–OH, C=O and O=C–OH (oxidative species) and the ratio to the C–C, C=C and –CH₂ (reductive species) species established in each case and the ratio was plotted in Fig. 2. The deconvoluted peaks centered at BE of 285.9, 287.6 and 289.1 eV were ascribed respectively to the C–OH, C=O and O=C–OH functional groups according to the BE reference values found in the literature for these functionalities [22,26,27,33,38,42–45]. The binding energy (BE) at 285.0 eV was assigned to the C–C, C=C and CH (reduced functionalities) to compute the ratio in the y-axis in Fig. 2.

The ratio of oxidized to reduced functionalities (COOH+COH/CH–; C–C) were seen to remain constant with RF-treatment time beyond 30 min. RF-plasma activated samples for 30 min were used in the experiments reported in Figs. 5 and 6 when assessing the *E. coli* inactivation kinetics. The lower trace in Fig. 2 shows the ratio of surface oxidized to the reduced functionalities when the RF-plasma was carried out at atmospheric pressure. A modest increase in the ratio oxidized surface groups/reduced groups was observed. In this case, the RF-pretreatment heated the

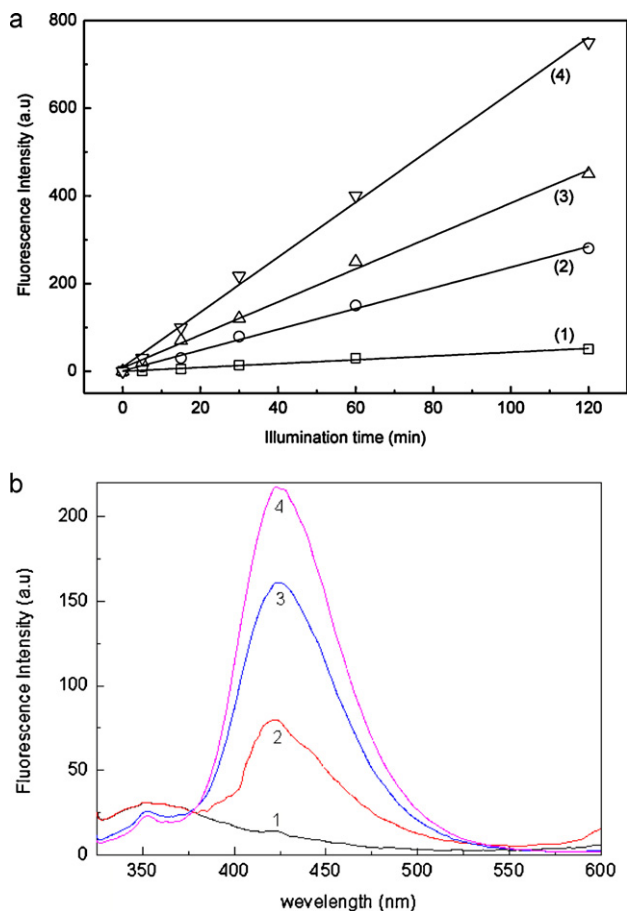


Fig. 3. (a) Fluorescence intensity vs irradiation time by means of a Osram Lumilux 18 W/827 actinic lamp up to 120 min for samples RF-pretreated for (1) zero, (2) 10 min, (3) 20 min and (4) 30 min. (b) Fluorescence intensity vs wavelength for RF-samples pretreated for (1) zero, (2) 10 min, (3) 20 min and (4) 30 min. All samples have been irradiated for 30 min by an Osram Lumilux 18 W/827 lamp. For other details see text.

polyester breaking intermolecular H-bonds and allows the introduction of oxidative functionalities [25,26,33]. Water evaporation is introduced on the polyester fibers by the RF-pretreatment. This allows for the diffusion of the TiO₂ into the polyester interior as a function of the RF-plasma pretreatment time (see Fig. 2).

3.2. Generation of the OH-radicals on TiO₂-polyester as a function irradiation time

Fig. 3a presents the increase in fluorescence of the polyester samples RF-plasma pretreated for 10, 20 and 30 min as a function of irradiation time up to 120 min by means Osram Lumilux 18 W/827 actinic. The results presented in Fig. 3b show the favorable effect of an increase RF-plasma pretreatment time up to 30 min on the polyester samples enhancing OH-radical generation upon illumination of the terephthalic acid. The OH-radicals produced on the TiO₂ coating have been quantified by measuring the fluorescence of the terephthalic acid [31,32]. Upon illumination, the terephthalic acid in NaOH solution converts on the TiO₂ coating to a highly fluorescent hydroxy-substituted product. Monitoring the increase of the hydroxy-product allows the estimation of the TiO₂ surface oxidative species, mainly the OH-radicals. We can only suggest that the active sites on the RF-pretreated TiO₂ coated polyester are introduced from two sources: (a) by the RF-pretreatment of the polyester generating oxidative functionalities as shown in Fig. 2 absorbing above 400 nm and (b) by the impurities, defects and

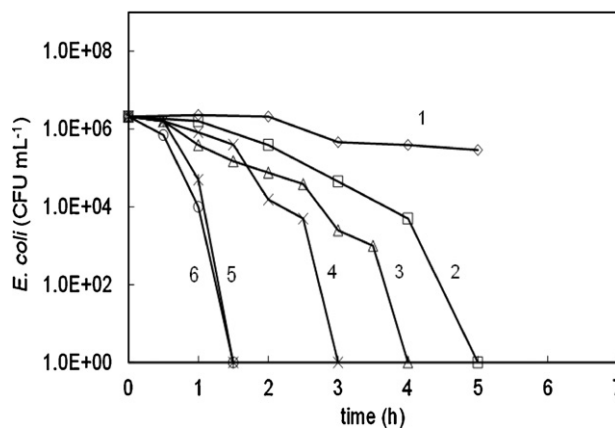


Fig. 4. *E. coli* inactivation kinetics of RF-plasma pretreated samples irradiated by actinic light for different times: (1) polyester alone, (2) TiO₂ coated, polyester not RF-plasma treated, (3) RF-plasma treated samples for: 10 min, (4) 20 min, (5) 30 min and (6) 120 min.

dangling bonds of the TiO₂ anatase crystallites of the colloidal coating shown in Fig. 8 absorbing in the visible range.

Fig. 3b presents the fluorescence intensity of polyester samples RF-pretreated for different times after 30 min illumination. The actinic lamp used to activate the fluorescence had an emission between 400 and 700 nm with an integral output of 1.1 mW/cm². The OH-radicals may photodegrade the polyester support during the photo-induced bacterial inactivation. In Fig. 7 below, up to the fifth cycle or the degradation kinetics kept constant suggesting that the polyester degradation did not occur during the initial sample recycling. We have applied SiO₂ films on textile below the TiO₂ surface film to avoid the corrosion of the textile substrate during the fabric self-cleaning processes coated with TiO₂ films [11].

3.3. Bacterial inactivation on RF-pretreated samples. About the effects of light dose, initial *E. coli* concentration and repetitive bacterial inactivation

Fig. 4 presents the *E. coli* inactivation kinetics by diverse RF-pretreated polyester samples. Under Osram Lumilux lamp irradiation tuned at a dose 4.1 mW/cm². Trace 1 presents the almost negligible disinfection action of the polyester sample by itself. Trace 2 shows a TiO₂-coated polyester without pretreatment inactivating bacteria within 5 h. Traces 3, 4 and 5 present a faster *E. coli* inactivation as the pretreatment time increases from 10 up to 30 min. Trace 6 shows that 120 min RF-pretreatment period does not further shorten the bacterial inactivation kinetics beyond the one shown by a 30 min RF-pretreatment. Therefore, the capacity to produce highly oxidative radicals (mainly OH-radicals) seems to reach a maximum after 30 min RF-plasma pretreatment as shown in Fig. 2 with respect to the data reported in Fig. 3a and b. Fig. 4 shows the fast bacterial inactivation due to the oxidative species induced under light on the TiO₂ as described in detail in Fig. 3a and b.

Fig. 5 presents the bacterial inactivation kinetics applying different light doses from an Osram 18 W/827 for three different light intensities. It is readily seen that the bacterial inactivation is strongly dependent on the light dose in the reactor cavity.

Fig. 6 shows the effect of the initial *E. coli* concentration on the bacterial inactivation kinetics. The time of inactivation as a function of the initial *E. coli* concentration was explored for the concentrations noted in the caption to Fig. 6. The time of inactivation was observed to decrease and become longer by a factor of almost three when the initial bacterial concentration was increased by ~3 orders of magnitude. This experiment was carried out to ensure that the present photocatalyst follows normal inactivation behavior when

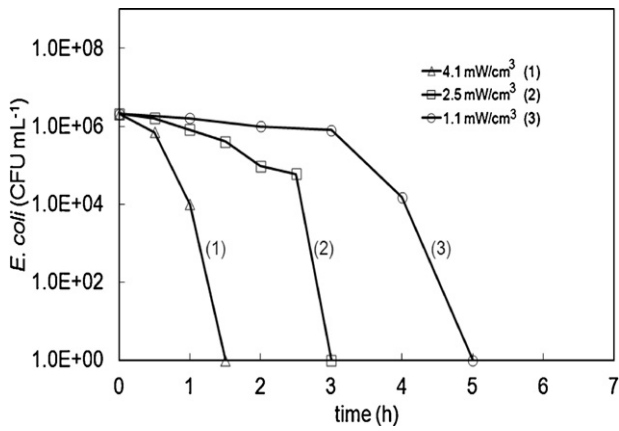


Fig. 5. Effect of light intensity on the bacterial inactivation kinetics applying light from an Osram Lumilux 18W/827 lamp on a RF-plasma pretreated sample for 30 min.

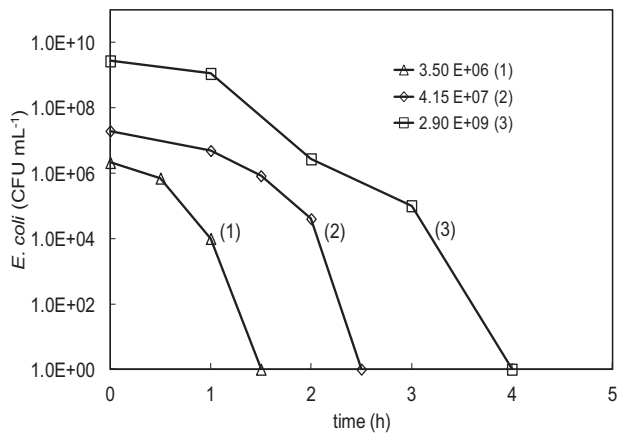


Fig. 6. Effect of the initial concentration of *E. coli* on the inactivation kinetics under light irradiation from an Osram Lumilux 18W/827 lamp using an RF-plasma pretreated sample for 30 min.

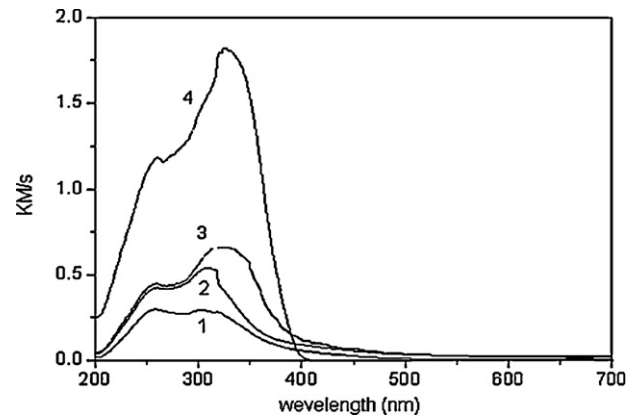


Fig. 8. Diffuse reflectance spectra (DRS) of TiO_2 -polyester samples RF-plasma pretreated for (1) zero, (2) 10 min, (3) 20 min and (4) 30 min.

interacting with *E. coli*, taken longer times to inactivate a higher initial CFU concentration.

Fig. 7 presents the repetitive *E. coli* inactivation by recycling of an RF-plasma pretreated for 30 min polyester- TiO_2 sample inactivating $\sim 7 \log_{10}$ bacteria under actinic light up to the 5th cycle within 1.5 h. It is readily seen that the initial bacterial inactivation conserves their kinetics validating the stability of the antibacterial activity of the TiO_2 -coatings.

3.4. Diffuse reflectance spectroscopy and visual perception of TiO_2 -polyester coated samples

The diffuse reflectance spectroscopy (DRS) of the RF pretreated samples for the 10, 20, 30 min polyester samples and the control sample are shown in Fig. 8. The spectra in Fig. 8 show the direct relation between the light absorption in Kubelka–Munk units and the RF-plasma pretreatment time. The rough UV–vis reflectance data cannot be used directly to assess the absorption coefficient of the RF-pretreated polyester because of the large scattering contribution to the reflectance spectra. Normally, a weak dependence is assumed for the scattering coefficient S on the wavelength. In

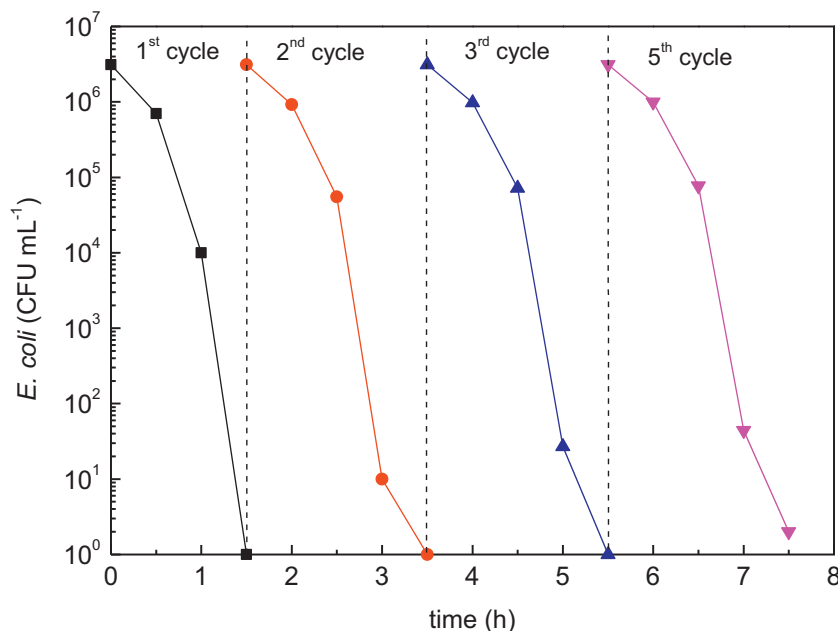


Fig. 7. Recycling of an RF-plasma 30 min pretreated sample loaded with TiO_2 under an Osram Lumilux 827/18W lamp up to the 5th cycle.

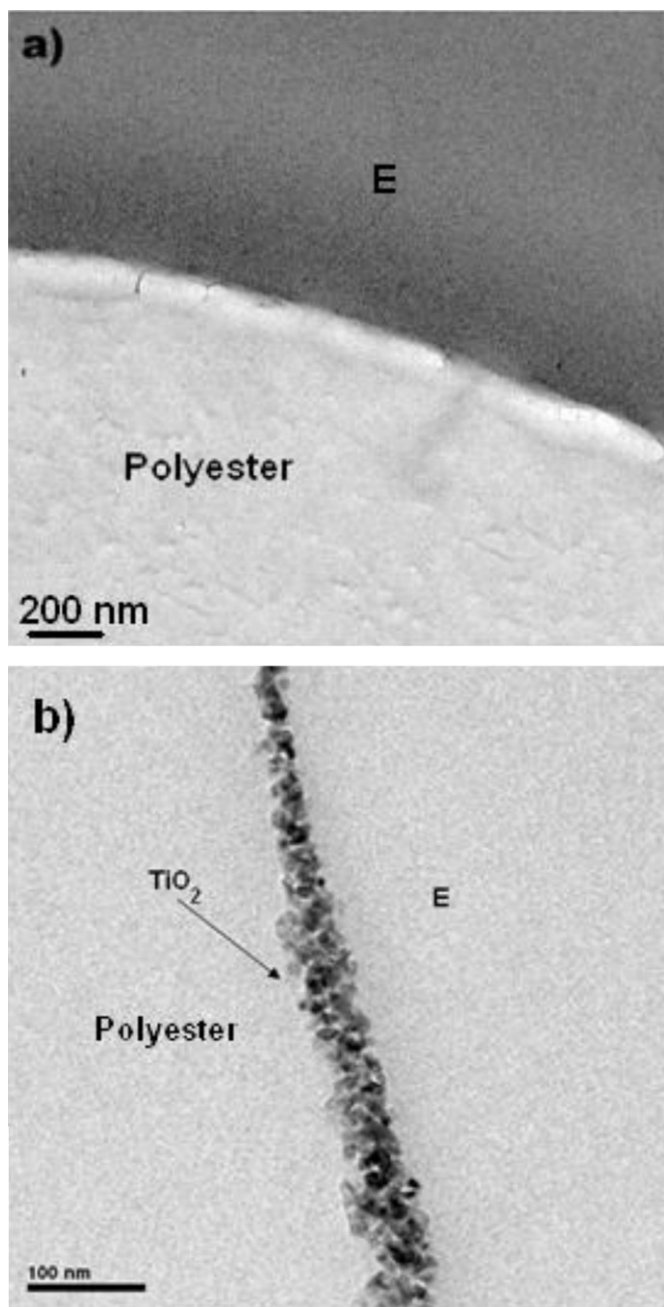


Fig. 9. Transmission electron microscopy of (a) polyester sample and (b) TiO₂-polyester RF-plasma pretreated for 30 min. E stands for epoxide used in the preparation and cutting of the sample.

Fig. 8, the scattering coefficient S is a function of the spectral wavelength in the DRS spectrum. The KM/S values for the samples in Fig. 8 follow the bacterial inactivation kinetics reported in Fig. 4.

The wt% Ti/wt polyester shown in Table 1 lends further support to the increased absorption of the samples as the Ti-content of the polyester increases. The absorption for the polyester alone is due to the TiO₂ used as whitener during the fabrication of the polyester described in Section 2.

3.5. Electron microscopy of samples (TEM) of TiO₂-polyester coated samples

Fig. 9 presents the TEM of (a) the polyester surface sample and (b) of the TiO₂ clusters on polyester forming a continuous coating

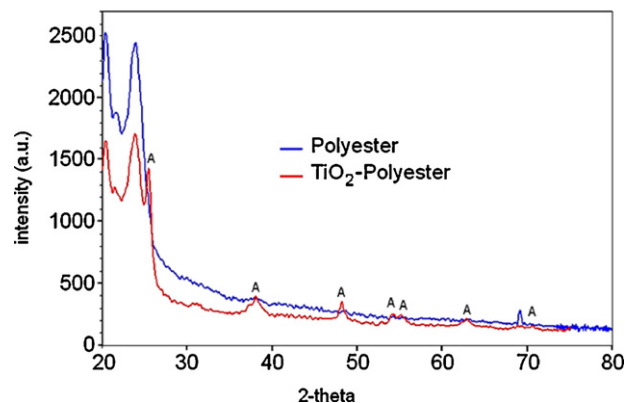


Fig. 10. X-ray diffraction of polyester sample used as reference (lower trace) and an RF-plasma sample pretreated for 30 min coated with TiO₂. For more details see text.

between 25 and 80 nm thick for an RF-plasma pretreated sample. The TiO₂ P-25 Degussa particles present sizes between 20 and 30 nm. This means that the coating in Fig. 9 comprise between one and four TiO₂ layers.

3.6. X-ray diffraction (XRD) of TiO₂ polyester samples

Fig. 10 shows the XRD for polyester and for polyester-TiO₂ loaded on a polyester sample RF-plasma pretreated for 30 min. The strong signal for anatase at 25.2° making up 80% of the TiO₂ Degussa P25 and the smaller anatase satellite peaks are seen in Fig. 10 the latter sample in the XRD spectrogram.

3.7. Contact angle (CA) determination of TiO₂ polyester samples

Fig. 11 shows the contact angle (CA) for the water droplet on polyester surface for the samples noted in the caption to Fig. 11. The sessile water drop disappears with time faster in the case of polyester than when the polyester has been RF-treated and subsequently coated with TiO₂. Although the polyester is hydrophobic, contact with water droplets shows the later effect due to high porosity (void areas) of the polyester allowing for water penetration through the polyester microstructure. The void areas are reduced by the addition of TiO₂ since it decreases the water penetration and concomitantly increasing the sample hydrophobicity.

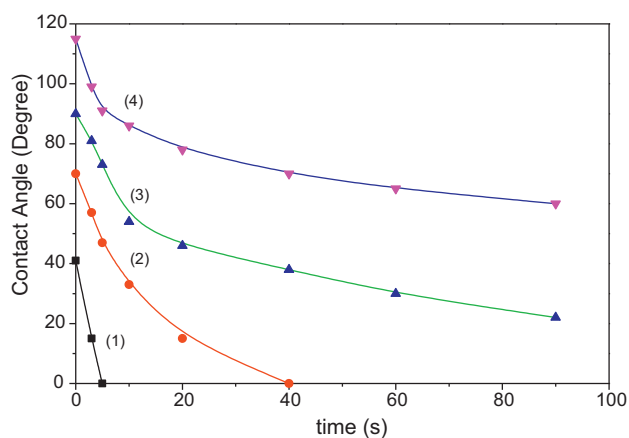


Fig. 11. Contact angle as a function of time for (1) polyester samples, (2) RF-plasma pretreated samples for 10 min, (3) RF-plasma pretreated samples for 20 min and (4) RF-plasma pretreated samples for 30 min.

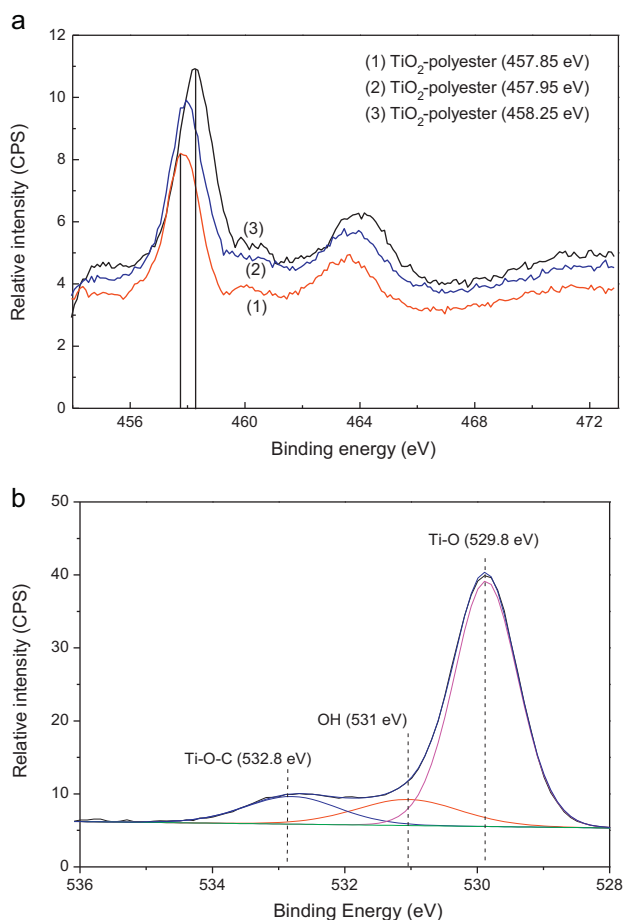


Fig. 12. (a) XPS $Ti2p_{3/2}$ peak shift in a sample RF-plasma pretreated for 30 min during *E. coli* inactivation: (1) at time zero, (2) at time 30 min and (3) at time 90 min. (b) XPS O1s spectra of RF-pretreated polyester loaded TiO_2 showing the Ti—O and Ti—O—C and the OH_{surf} surface groups.

3.8. X-ray photoelectron microscopy of samples (XPS) of polyester and of TiO_2 polyester sample

Fig. 12a presents the $Ti2p_{3/2}$ peak at time zero shifting during the bacterial inactivation to 458.25 eV. This is the evidence for a Ti^{4+}/Ti^{3+} redox reactions taking place on the TiO_2 polyester surface in contact with surface bacteria. Shifts in the XPS peaks ≥ 0.2 eV reflect valid changes in the oxidation states of the elements [38]. Table 2 shows the surface atomic concentration on an RF-plasma pretreated sample of 30 min during bacterial inactivation under actinic light irradiation. The rapid destruction of C generated by the bacterial destruction for samples contacted with bacteria is proven by the sample C-concentration after the 3 s contact with the sample surface. O, N and Ti are seen to remain constant up to 90 min.

Fig. 12b shows the deconvoluted spectrum of a RF-plasma pretreated polyester sample TiO_2 coated showing the OH-group at

Table 2

Surface percentage atomic concentration of TiO_2 -coated polyester during *E. coli* inactivation as determined by XPS. The first row refers to a sample not contacted with bacteria.

| Sample identifier | C | O | N | Ti |
|-------------------|-------|-------|------|-------|
| 0 | 28.51 | 51.23 | 0.36 | 19.9 |
| 3 s | 48.06 | 37.68 | 1.02 | 13.24 |
| 30 min | 50.32 | 36.59 | 1.05 | 12.04 |
| 60 min | 52.14 | 36.95 | 0.37 | 10.46 |
| 90 min | 52.85 | 36.42 | 0.39 | 10.34 |

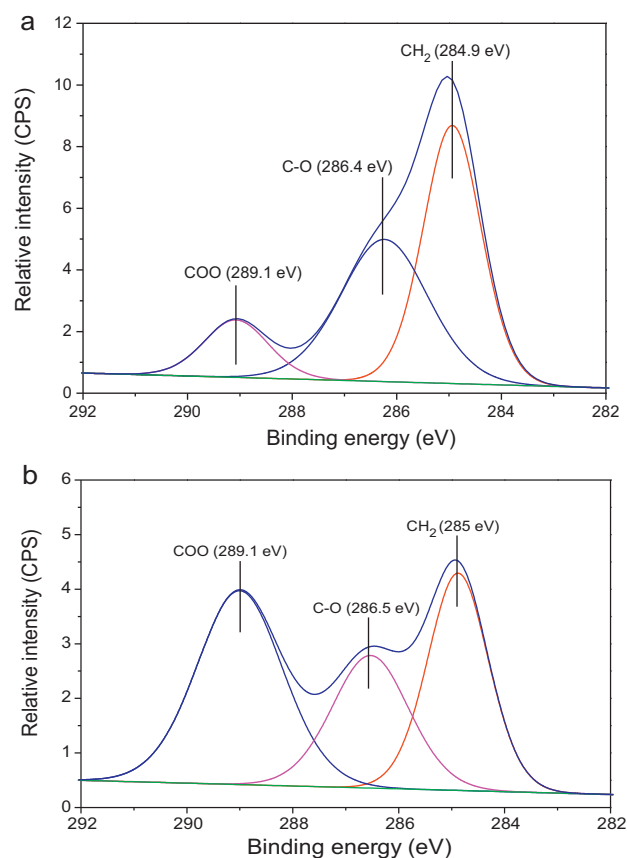


Fig. 13. XPS C1s spectra of (a) untreated polyester and (b) RF-plasma pretreated polyester for 30 min.

531.0 eV [28] and the Ti—O at 529.8 eV [38] and the Ti—O—C peak at 532.8 eV [37]. A large amount of adsorbed/chemisorbed water was introduced in the sample during the sol-gel coating at temperatures no higher than 100 °C. The amount of surface OH_{surf} radical adsorbed on the sample is higher after the RF-plasma pretreatment (data not shown) due to the increased hydrophilicity introduced by the O-containing polar groups by the RF-plasma pretreatment.

Fig. 13a shows the XPS spectra for the untreated C1s signal region. The peak of the untreated polyester is deconvoluted into components: the peak at 285 eV assigned to the CH_2 - functionality, and the peaks at 286.5 eV and 289 eV assigned the C—O and COO- functionalities respectively. Fig. 13b shows that after 30 min RF-plasma pretreatment, the area peaks for C—O and COO- increase, compared to the untreated sample. At the same time, the relative number of CH_2 - groups decreased. This indicates that some CH_2 - groups have been oxidized to COOH or COH.

Fig. 14a shows the XPS spectra collected from the untreated and RF-plasma pretreated samples for 30 min in the O1s XPS spectral region. The two O1s peaks are fitted with two main peaks at energies of 533.6 eV and 532.0 eV. In addition, the O1s peak from the untreated sample shows a shoulder on the low energy side at 530.5 eV [33] and the O1s peak from the treated sample shows a shoulder on at 535.8 eV. The peak at 532.0 eV corresponds to oxygen atoms attached to C in the form of COO groups, while the peak at 533.5 eV corresponds to the oxygen atoms attached singly to carbon. The increased intensity of the areas under the peak at 533.5 eV and at 532 eV shows that COH increases for the RF-plasma pretreated samples. A concomitant increase of H_2O/OH_{surf} molecules on the surface was observed (data not shown) due to the high surface energy of the film in the RF-pretreated samples.

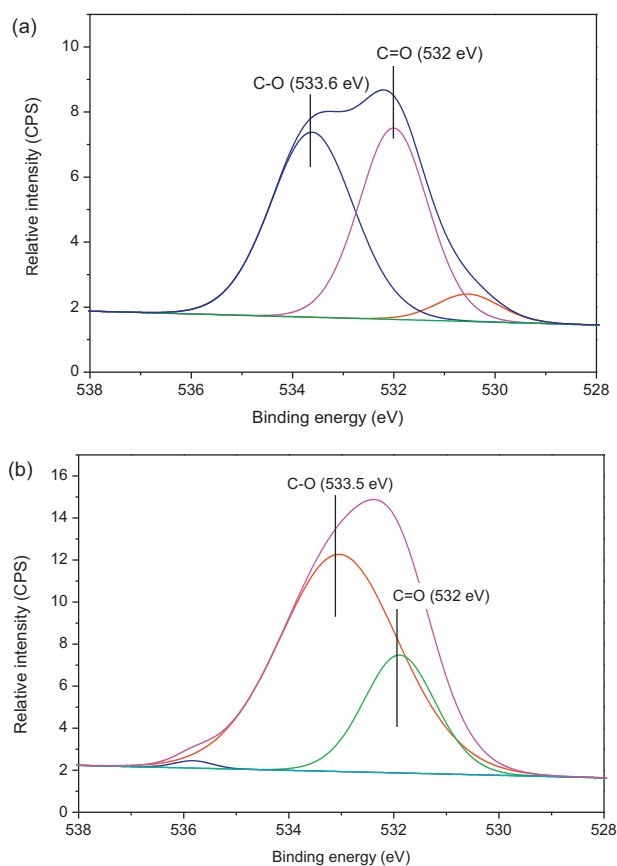


Fig. 14. XPS O1s spectra of (a) untreated polyester and (b) RF-plasma pretreated polyester for 120 min.

4. Conclusion

RF-plasma is shown to be a useful pretreatment method to increase the number of active sites and bondability on the polyester surface allowing for a much higher TiO₂ loading on the textile compared to non-pretreated samples. The pretreated samples accelerate significantly *E. coli* inactivation reducing by a factor of >3 the bacterial inactivation time compared to non-pretreated polyester TiO₂ samples. The polyester RF-plasma pretreatment induced modifications of the surface ratio of oxidative and reductive species in the polyester surface as detected by XPS. Oxidative species (mainly OH-radicals) were identified on the irradiated polyester-TiO₂ samples and a higher amount of oxidative species lead to a faster bacterial inactivation. TEM of the RF-plasma pretreated polyester shows a continuous microstructure for the TiO₂ coating on the polyester surface. By XPS, self-cleaning of the bacterial inactivation residues on the polyester-TiO₂ was confirmed which enables the sample to inactivate a new bacterial charge at the end of the disinfection process.

Acknowledgments

We thank the COST Action MP0804 Highly Ionized Pulse Plasma Processes (HIPIMS), The Swiss-Hungarian Cooperation Program “Sustainable fine chemicals pharmaceutical industry: screening and utilization of liquid wastes” and the EPFL for the support of this work.

References

- [1] A. Fujishima, K. Hashimoto, T. Watanabe, TiO₂ Photocatalysis, Bkc Inc. Pub. Co., Tokyo, 2004.
- [2] A. Mills, S. Lee, Journal of Photochemistry and Photobiology A 152 (2002) 1.
- [3] K. Page, M. Wilson, I.P. Parkin, Journal of Materials Chemistry 19 (2009) 3819–3831.
- [4] S. Noimark, Ch. Dunhill, M. Wilson, I.P. Parkin, Chemical Society Reviews 38 (2009) 3435–3448.
- [5] S. Pigeot-Rémy, F. Simonet, E. Errazuriz Cerda, J.V. Lazzaroni, D. Atlan, C. Guillard, Applied Catalysis B 104 (2011) 390–398.
- [6] S. Dancer, Journal of Hospital Infection 73 (2009) 378–385.
- [7] A. Kramer, I. Schwebke, G. Kampf, BMC Infectious Diseases 6 (2006) 130–139.
- [8] J. Kiwi, V. Nadtochenko, Journal of Physical Chemistry B 108 (2004) 17675–17684.
- [9] D. Gumy, C. Pulgarin, C. Morais, P. Bowen, J. Kiwi, Applied Catalysis B 63 (63) (2005) 76–84.
- [10] A.G. Rincon, C. Pulgarin, Applied Catalysis B 44 (2003) 263–270.
- [11] J. Kiwi, C. Pulgarin, Catalysis Today 151 (2010) 2–7 (and references therein).
- [12] H. Pant, D. Pandeya, K. Nam, W. Baek, S. Hong, H. Kim, Journal of Hazardous Materials 189 (2011) 465–471.
- [13] O. Akhavan, E. Ghaderi, Surface and Coatings Technology 204 (2010) 3676–3683.
- [14] H. Kong, J. Song, J. Jang, Environmental Science and Technology 44 (2010) 5672–5676.
- [15] W. Su, S. Wang, X. Wang, X. Fu, J. Weng, Surface and Coatings Technology 205 (2010) 465–469.
- [16] G. Jiang, J. Zeng, Journal of Applied Polymer Science 116 (2010) 779–784.
- [17] O. Akhavan, Journal of Colloid and Interface Science 336 (2009) 117–124.
- [18] D. Mihailovic, Z. Saponjic, M. Radojicic, T. Radetic, J. Jovancic, M. Nedeljkovic, M. Radetic, Carbohydrate Polymers 79 (2010) 526–532.
- [19] M. Radetic, V. Ilic, V. Vodnik, S. Dimitrijevic, P. Jovancic, Z. Saponjic, J. Nedeljkovic, Polymers for Advanced Technologies 19 (2008) 1816–1821.
- [20] D. Hegemann, M. Hossain, M. Balazs, Progress in Organic Coatings 58 (2007) 237–240.
- [21] D. Hegemann, M. Amberg, A. Ritter, M. Heuberger, Materials and Technology 24 (2009) 41–45.
- [22] J. Kasanen, M. Suvanto, Z. Pakkanen, Journal of Applied Polymer Science 111 (2007) 2597–2602.
- [23] T. Yuranova, A.-G. Rincon, A. Bozzi, S. Parra, C. Pulgarin, A. Albers, J. Kiwi, Journal of Photochemistry and Photobiology A: Chemistry 161 (2003) 27–34.
- [24] A. Bozzi, T. Yuranova, J. Kiwi, Journal of Photochemistry and Photobiology A: Chemistry 172 (2005) 27–34.
- [25] M.I. Mejía, J.M. Marín, G. Restrepo, C. Pulgarin, E. Mielczarski, J. Mielczarski, J. Kiwi, ACS Applied Materials and Interfaces 1 (2009) 2190–2198.
- [26] M.I. Mejía, J.M. Marín, G. Restrepo, C. Pulgarin, E. Mielczarski, J. Mielczarski, Y. Arroyo, J.-C. Lavanchy, J. Kiwi, Applied Catalysis B 91 (2009) 481–488.
- [27] A. Torres, C. Ruales, C. Pulgarin, C. Aimable, P. Bowen, V. Sarria, ACS Applied Materials and Interfaces 2 (2010) 2547–2552.
- [28] C. Chan, T. Ko, H. Hiroaka, Surface Science Reports 24 (1996) 1–54.
- [29] A. Kinloch, Adhesion and Adhesives, Chapman and Hall Inc., New York, USA, 1987.
- [30] M. Willert-Porada, 8th International Conference on Microwave and High-Frequency Heating, Germany, 2001, pp. 440–443.
- [31] X. Li, Y. Oiu, Applied Surface Science 258 (2012) 7787–7793.
- [32] A. Johnson, The Theory of Coloration of Textiles, Society of Dyes and Colourists, Bradford, UK, 1983.
- [33] M. Dhananjeyan, E. Mielczarski, K. Thampi, Ph. Buffat, M. Bensimon, A. Kulik, J. Mielczarski, J. Kiwi, Journal of Physical Chemistry B 105 (2001) 12046–12055.
- [34] S. Wu, Polymer Interface and Adhesion, Marcel Dekker, New York, 1992.
- [35] Thüringer Surface and Biomaterials Kolloquium, Zeulenroda, Germany, 13–15 September 2012.
- [36] D. Wu, M. Long, J. Zhou, W. Cai, X. Zhu, C. Chen, Y. Wu, Surface and Coatings Technology 203 (2009) 3728–3733.
- [37] M. Dhananjeyan, J. Kiwi, R. Thampi, Chemical Communications (2000) 1443–1444.
- [38] C.D. Wagner, M.W. Riggs, E.L. Davis, G.E. Müllenberg (Eds.), Handbook of X-ray Photoelectron Spectroscopy, Perkin-Elmer Corporation Physical Electronics Division, Minnesota, 1979.
- [39] A.D. Shirley, Physical Reviews B5 (1972) 4709–4716.
- [40] K. Ishibashi, A. Fujishima, T. Watanabe, K. Hashimoto, Electrochemistry Communications 2 (2009) 207–210.
- [41] F. Liu, C. Roussel, G. Lagger, P. Tacchini, H. Girault, Analytical Chemistry 77 (2005) 7687–7694.
- [42] S. Yumitori, Journal of Materials Science 35 (2000) 139–146.
- [43] R. Dastjerdi, M. Montazer, Th. Stegmaier, M. Moghadm, Colloids and Surfaces B: Biointerfaces 91 (2012) 280–290.
- [44] H. Yaghoobi, N. Thagavinia, K. Alamdari, A. Volinsky, ACS Applied Materials and Interfaces 2 (2010) 2629–2636.
- [45] O. Akhavan, R. Azimirad, S. Safa, M.M. Larijani, Journal of Materials Chemistry 20 (2010) 7386–7392.